PCCP

ROYAL SOCIETY OF CHEMISTRY

PAPER

View Article Online
View Journal | View Issue

Cite this: *Phys. Chem. Chem. Phys.*, 2024, **26**, 27902

Reinvestigation of the ν_3–ν_6 Coriolis interaction in trifluoroiodomethane†

Arun Bhujel, ‡[a] Salma Akter, ‡[a] Muhammad Qasim Ali [a] and G. Barratt Park *[ab]

Received 3rd July 2024,
Accepted 21st October 2024

DOI: 10.1039/d4cp02640c

rsc.li/pccp

The lowest-frequency fundamental ν_6 of trifluoroiodomethane (CF_3I) has never been directly observed and analyzed at high resolution in the gas phase. The ν_6(e) level interacts with ν_3(a_1) at 286.297 cm^{-1} *via* a *b*-axis Coriolis interaction, which perturbs the rotational structure of both levels. In this work, we report low-*J* microwave transitions (for *J* ranging from 0–2) within the ν_6 vibrational level. The *l*-type doubling observed in our spectrum agreed poorly with the predictions of previously published models of the interacting ν_3–ν_6 levels, prompting us to refine the model. We performed *ab initio* anharmonic force-field calculations, which were used to constrain some of the parameters, and which served as a check on some of the floated parameters. We fit a dataset consisting of 3593 transitions, which combined our measurements with previous microwave, millimeter wave, and high-resolution infrared observations. A reasonable set of fit parameters is obtained with ν_6 = 267.28 cm^{-1}, but we cannot rule out a lower value of ν_6 = 261.5 cm^{-1} consistent with analyses of the vibrational level structure.

Introduction

Trifluoroiodomethane (CF_3I) has potential as a more environmentally friendly alternative to Halon 1301 (CF_3Br) as a fire suppressant, since its ozone depleting potential is lower by a factor of ~1000.[1] CF_3I has also been used in trifluoromethylation reactions[2] and multiphoton dissociation experiments.[3] The frequency of its lowest-lying fundamental, ν_6(e) was the subject of some controversy in the early IR and Raman work because the ν_6 fundamental transition is relatively weak and is poorly resolved from the stronger ν_3(a_1) fundamental.[4–9] Values reported for the ν_3 – ν_6 frequency difference range from 19–28 cm^{-1}. A number of microwave studies have been reported on CF_3I in its ground vibrational state.[8,10–14] A millimeter-wave study by Walters and Whiffen[15] led to the assignment of rotational transitions in the excited ν_6 and ν_3 vibrational levels and enabled a characterization of the *b*-axis Coriolis interaction between the ν_6 and ν_3 levels. This analysis favored a low value of $\nu_3 - \nu_6 = 19 \pm 2$ cm^{-1}. On the other hand, careful assessment of the vibrational level structure has led to a value of $\nu_3 - \nu_6 = 24.8 \pm 1.5$ cm^{-1}.[16]

Subsequent high-resolution spectroscopic investigations include a microwave study by Gerke and Harder[17] in which direct *l*-type doubling transitions are reported for the ν_6 level in the J = 40–51 range. These authors reported parameters for the off-diagonal spin-rotation interaction with $\Delta l = \Delta K = \pm 2$ selection rules. The hyperfine structure probed in this work is also highly sensitive to the *b*-axis Coriolis interaction with the ν_3 level, but the authors made no attempt to deperturb Coriolis contributions, using instead effective values for the q^+ and q_J *l*-type doubling constants.

In another study by Willaert *et al.*,[18] a high-resolution infrared spectrum of the ν_3 fundamental band was recorded at 0.001 cm^{-1} resolution using synchrotron sources. These authors searched for the ν_6 fundamental but could not detect it due to its extremely weak transition strength. The authors estimated an upper limit of 7.5 m mol^{-1} for the integrated cross section of the ν_6 band. Three different fit models were used to interpret the results. In the preliminary analysis, ν_3 was considered to be an isolated state, and its perturbed rotational structure was fitted with the help of high-order centrifugal distortion parameters that effectively account for the Coriolis interaction with ν_6. The Coriolis interaction was taken into account explicitly in two additional models, which were fit to combined datasets that included microwave and millimeter wave transitions[15,17] within modes ν_3 and ν_6 in addition to the ν_3 IR data.[18] In the first model, the ν_6 origin was fixed to the value reported by Walters and Whiffen[15] and the A_6 rotational constant was constrained to equal the A_3 rotational constant. (Here, subscripts refer to the rotational parameters for the ν_6

[a] *Department of Chemistry and Biochemistry, Texas Tech University, Lubbock, Texas 79409, USA. E-mail: barratt.park@ttu.edu*
[b] *Department of Dynamics at Surfaces, Max Planck Institute for Multidisciplinary Sciences, Göttingen 37077, Germany*

† Electronic supplementary information (ESI) available. See DOI: https://doi.org/10.1039/d4cp02640c

‡ These authors contributed equally.

and ν_3 fundamental vibrational levels, respectively.) In the second model, the ν_6 origin was fixed to the value reported by Bürger *et al.*[16] Both fits required the inclusion of high-order C_B^J and C_B^K Coriolis constants that correct for the *J*- and *K*-dependence of the Coriolis zeta parameter, respectively. The first fit had the unusual feature that the q^+ *l*-type doubling constant for ν_6 was not well determined, but it was necessary to include higher order q_J and q_K corrections that account for the *J*- and *K*-dependence of the *l*-type doubling.

In this work, we have used CF_3I as a test molecule for evaluation of a newly constructed chirped-pulse Fourier-transform microwave (CP-FTMW) spectrometer,[19,20] operating in the 2–8 GHz region. We found expansion conditions that favored the generation of CF_3I in the excited ν_6 vibrational state, enabling measurements of the J = 1–0 and J = 2–1 spectral regions. The spectrum exhibits structure due to the large nuclear quadrupole coupling constant arising from the ^{127}I nucleus as well as *l*-type doubling that arises from the doubly degenerate vibration. Our measured frequencies agree poorly with the predictions of spectroscopic constants for the interacting ν_6 and ν_3 levels reported from the millimeter-wave work of Walters and Whiffen[15] and the IR study of Willaert *et al.*,[18] which motivated us to re-evaluate the fit model. We report the results of fitting our updated model to a combined dataset that includes all microwave, millimeter-wave, and IR transition frequencies reported here and in ref. 15, 17 and 18. Our fit model is guided by the results of *ab initio* anharmonic force field calculations.

Experimental

A schematic diagram of the newly constructed microwave spectrometer is shown in Fig. 1. The design is based on the compact 2–8 GHz spectrometer reported by Neill *et al.*[21] A chirped excitation pulse is produced by an arbitrary waveform generator (AWG, Tektronix 710B). The frequency and bandwidth of the pulse are multiplied by four using an active quadrupler that was constructed from surplus parts. The resulting chirped pulse is amplified by a 10 W solid state amplifier (RF-Lambda, RFLUPA01G09GA) and coupled into free space by a high gain antenna (ATM 250-441EM-NF). A single-pole single-throw (SPST, KDI SW-2018AC) switch is used on the output of the amplifier to reduce the noise floor during signal collection. The free induction decay (FID) emitted by the sample is collected by a matched antenna and sent through a low-noise amplifier (LNA, RF-Lambda RLNA02G08G30D). The LNA is protected from the excitation pulse by a limiter (CAES ACLM-4601) and a SPST switch (KDI SW-2018AC). Finally, the FID is down-converted in a mixer (Watkins Johnson M93C) using a 4 GHz phase-locked oscillator (Lotus Systems) as the LO, and the FID is averaged in the time domain on a 2.5 GHz oscilloscope (Teledyne Lecroy WavePro 254HD) operating at a 20 GS per s sampling rate. A 10 MHz rubidium oscillator (SRS FS725) is used to provide phase stability and frequency accuracy. We are currently in the process of upgrading the oscilloscope to the full bandwidth of 8 GHz, and we plan to make additional modifications to improve the spectrometer's sensitivity.

We found that population of the excited ν_6 state was favored by expansion of CF_3I in Ar with mixing ratios in the range of 1–10%. The ν_6 lines were absent when N_2 was used as the seed gas, and they were also not observed in a previously reported spectrum[22] using Ne. Spectra of CF_3I were acquired for a 10% CF_3I/Ar mixture. CF_3I (99% purity) was obtained from Sigma Aldrich and used without further purification. The sample was placed in a stainless-steel reservoir at room temperature and was expanded into a four-way cross vacuum chamber through a pulsed nozzle (Ideal Vacuum Pulse Valve, P1010774) at a backing pressure of 1 bar and a repetition rate of 20 Hz. The vacuum

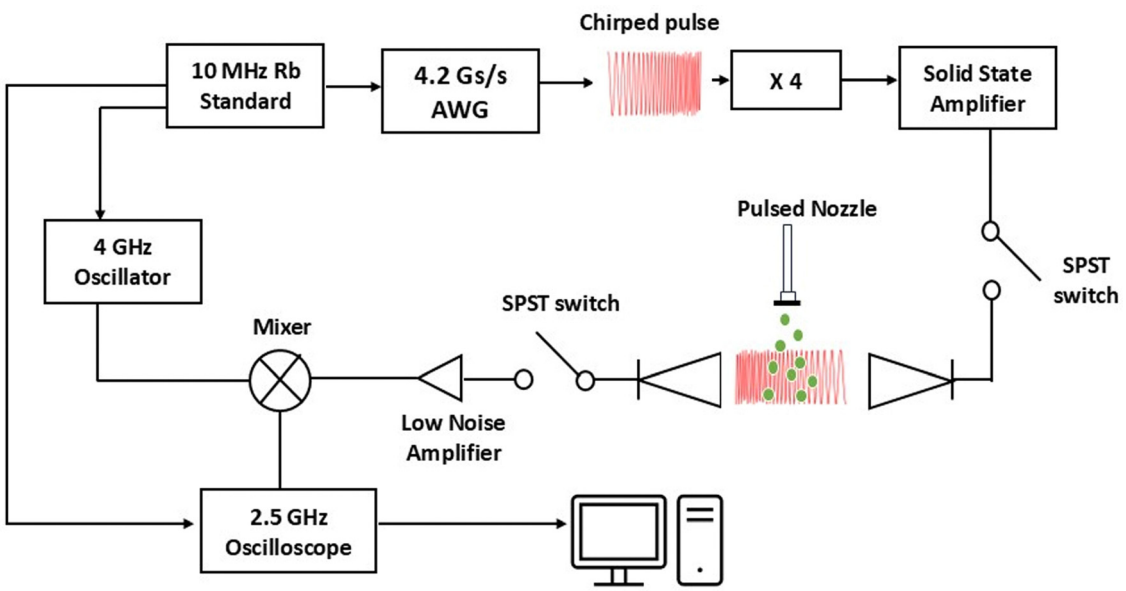

Fig. 1 Schematic design of the 2–8 GHz CP-FTMW spectrometer.

Table 1 Ground-state rotational constants, vibration-rotation constants, and fundamental vibrational frequencies of $^{12}CF_3I$, obtained from *ab initio* anharmonic force field calculations are compared with experimental values. For the experimental ν_6 fundamental frequency, we include the value obtained in this work from a model of the ν_3–ν_6 Coriolis interaction as well as the value recommended in ref. 16, which is based on a comprehensive vibrational analysis, including the energetic positions of overtone and combination levels

	HF			MP2			CCSD			
Param.	3-21G	6-311G	6-311G**	3-21G	6-311G	6-311G**	3-21G	6-311G	6-311G**	Expt.
A_0/MHz	5607.00	5546.54	5911.00	5365.13	5215.47	5692.53	5382.05	5254.75	5722.32	5759.01[a]
B_0/MHz	1470.47	1493.24	1524.95	1428.16	1452.68	1497.95	1423.70	1449.31	1494.97	1523.28287(2)[b]
$\alpha_6^{(A)}$/MHz	−7.46	−6.88	−7.85	−7.17	−6.16	−7.72	−7.36	−6.46	−7.86	
$\alpha_6^{(B)}$/MHz	0.764	0.696	0.675	1.033	0.782	0.842	1.105	0.862	0.853	1.36254(21)[c]
$\alpha_3^{(A)}$/MHz	0.357	0.399	0.246	0.522	0.531	0.402	0.525	0.489	0.375	0.4254(25)[c]
$\alpha_3^{(B)}$/MHz	2.58	2.38	2.76	3.29	2.66	3.35	3.40	2.77	3.30	3.5822(3)[c]
ν_1/cm^{-1}	1169.50	1142.05	1182.10	1061.05	1011.13	1072.40				1076.0551(1)[d]
ν_2/cm^{-1}	748.33	733.51	814.88	689.90	655.77	748.28				743.36912(12)[e]
ν_3/cm^{-1}	296.90	306.14	309.21	269.78	284.94	284.58				286.297298(32)[c]
ν_4/cm^{-1}	1361.69	1229.61	1337.79	1242.26	1068.49	1214.01				1187.62771(5)[f]
ν_5/cm^{-1}	539.93	525.16	577.91	501.41	467.79	538.06				539.830(7)[g]
ν_6/cm^{-1}	277.81	283.10	296.59	259.38	263.04	276.20				267.28155(33)[c] 261.5(15)[g]

[a] Ref. 25. [b] Ref. 14. [c] This work. [d] Ref. 26. [e] Ref. 27. [f] Ref. 28. [g] Ref. 16.

chamber is evacuated by a diffusion pump (Varian VHS-6) to a baseline pressure of $\sim 10^{-7}$ mbar.

Calculations

The minimum energy geometry and force field of CF_3I was calculated using the CFOUR package.[23] Calculations were performed at the MP2, CCSD, and CCSD(T) levels of theory with a series of Pople basis sets extending up to 6-311G**.[24] At the CCSD(T) level of theory, only the harmonic force field was calculated. At the MP2 and CCSD levels of theory, the cubic anharmonic force field was calculated, allowing calculations of fundamental vibrational frequencies and vibration-rotation constants. At this level of theory, the vibrational frequencies and the absolute rotational constants are not expected to be spectroscopically accurate. However, the vibration-rotation constants (α values), can be significantly more reliable than the

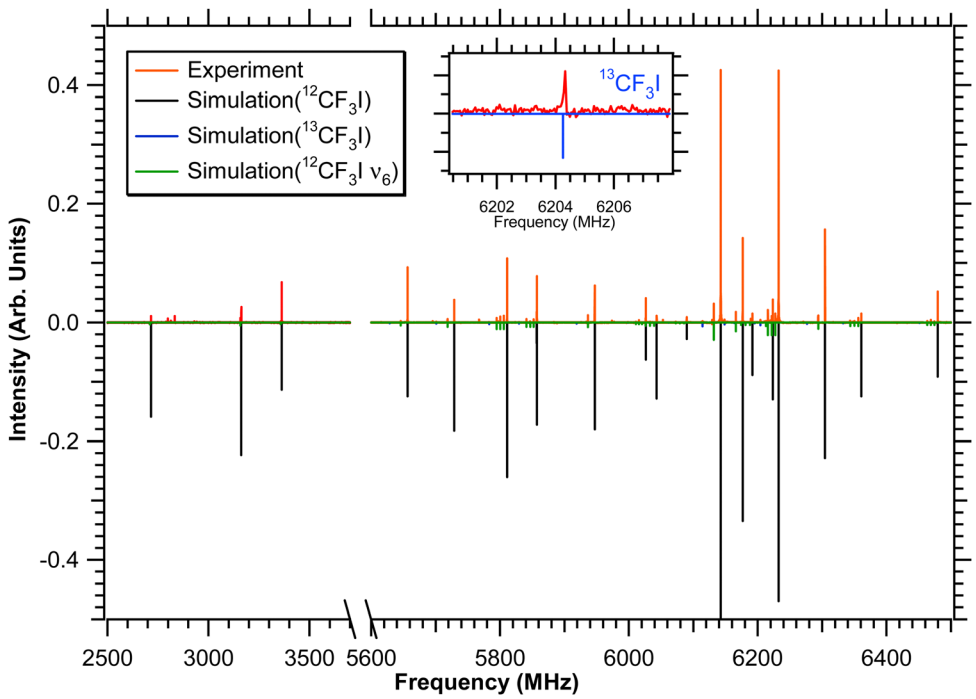

Fig. 2 2–8 GHz spectrum of CF_3I. The spectrum contains lines in two different regions: J = 0 to 1 transitions lie in the 2500–3500 MHz range and J = 1 to 2 transitions lie in the 5600–6500 MHz range. The measured spectrum (red, upward directed peaks) is compared to simulated line frequencies and intensities (downward directed peaks, see legend). The inset shows the (J,K,F) = (2,1,4.5) ← (1,1,3.5) transition of the $^{13}CF_3I$ isotopologue, obtained in natural abundance.

absolute rotational constants. Quartic centrifugal distortion constants and Coriolis zeta constants can be calculated quite accurately from the harmonic force field and can be meaningfully compared with (deperturbed) experimental values. The calculated rotational constants, vibration-rotation constants, and fundamental frequencies are given in Table 1. Experimental values are shown for comparison. Calculated geometries are given in Table S1 (ESI†), and calculated centrifugal distortion constants and Coriolis zeta constants are given in Table S2 of the ESI.†

Results

Fig. 2 shows an overview of the 2–8 GHz spectrum of CF_3I. The spectrum was acquired at a resolution of 50 kHz with a total of 600 000 averages for both signal and background with total acquisition time of around 17 hours. In addition to the strong lines from the CF_3I ground state, we also observe lines from the $^{13}CF_3I$ isotopologue (Fig. 2 inset) in natural abundance and arising from the vibrationally excited ν_6 level of $^{12}CF_3I$. The simulated frequencies and intensities were calculated using the SPCAT/SPFIT suite[29] and are shown for comparison in Fig. 2. The frequencies of $^{13}CF_3I$ lines and vibrational satellites have not been previously reported in this frequency range and are listed in Table 2.

The most recently reported spectroscopic constants for ground-state $^{12}CF_3I$[14] and $^{13}CF_3I$[15] were in good agreement with our observation, so we made no attempts to fit these datasets. However, the predicted line positions for the ν_6 vibrational satellites deviated significantly from the prediction calculated using the parameters of Walters and Whiffen[15] and from the prediction calculated using the parameters of Willaert *et al.*[18] (Fig. 3A). The splitting between the *l*-type doubled $k = 1$ satellites that arise from transitions between A_1 and A_2 rovibrational species exhibited particularly poor agreement. We therefore re-evaluated the spectroscopic constants using two different models. In the first model, we considered ν_6 as an isolated state, and we fit a combined dataset consisting of our microwave measurements, the millimeter-wave measurements of Walters and Whiffen,[30] and the *l*-type doubling transitions of Gerke and Harder.[17] We found that the introduction of the $eQq\eta$ parameter allowed our low-J data to be fit adequately. This parameter[31] can be thought of as a vibrationally induced asymmetry in the χ_{bb} and χ_{cc} components of the nuclear quadrupole coupling tensor, which gives rise to $\Delta K = \pm 2$, $\Delta l = \pm 2$ matrix elements and allows the effective *l*-type doubling to depend rather strongly on the nuclear spin state. It was also necessary to include the C_6 spin-rotation interaction parameter to obtain a proper fit to the *l*-type doubling transitions. The fit results are shown in Table 3. Most of the parameters obtained were similar to those obtained by Walters and Whiffen. The q_J, $eQq\eta$, and C_6 parameters were similar to those reported by Gerke and Harder. The overall rms error was 0.083 MHz. However, it is important to consider that the various sources of data spanned a large range of measurement accuracies, so it was important to weight each observed frequency according to the stated measurement uncertainty. A summary of the rms fit error obtained from each dataset is given at the bottom of Table 3. Note that the rms fit errors are in quite reasonable agreement with the respective measurement uncertainties.

We performed a second fit that explicitly accounts for the Coriolis interaction between the ν_3 and ν_6 levels. We fit a combined dataset of 3593 frequencies, which included all the ν_6 microwave transitions used in the first fit as well as 137 ν_3 millimeter wave transitions from ref. 30 and 3053 ν_3 fundamental IR transitions from ref. 18. It is challenging to model such an interaction given that the precise ν_6 fundamental frequency is unknown. Even a handful of rotationally resolved ν_6 fundamental IR transitions would enable significantly more constraints to be placed on the fit model. Not only would such data provide the ν_3–ν_6 energetic separation, the perpendicular ν_6 fundamental transition would also provide information about the A_6 rotational constant and the D_k centrifugal distortion constant, both of which are correlated to other fitting parameters. For example, in the most recent attempt by Willaert *et al.*[18] to fit the interaction, two different fits were

Table 2 The upper section lists $^{13}CF_3I$ lines. The Obs−Calc residuals are obtained using the parameters of ref. 15. Frequencies are given in units of MHz. The lower section lists observed transitions in the $\nu_6 = 1$, $l = \pm 1$ vibrational state. The Obs−Calc residuals are from the fit parameters given in Table 4. Frequencies are given in units of MHz

J'	K'	F'	J''	K''	F''	Obs freq	Obs−Calc
2	0	3.5	1	0	3.5	5700.838	−0.118
2	1	3.5	1	1	2.5	5782.983	−0.079
2	0	2.5	1	0	3.5	5829.291	−0.051
2	0	4.5	1	0	3.5	6114.379	0.007
2	0	3.5	1	0	2.5	6148.549	0.048
2	1	4.5	1	1	3.5	6204.338	0.081

J'	K'	l'	F'	sym′	J''	K''	l''	F''	sym″	Obs freq	Obs–Calc
1	0		3.5	E	0	0		2.5	E	3157.4967	0.0348
1	0		1.5	E	0	0		1.5	E	3357.7249	−0.0421
2	0		2.5	E	1	0		1.5	E	5645.9870	−0.0055
2	0		3.5	E	1	0		3.5	E	5718.3919	0.0033
2	1	1	3.5	A_1	1	1	1	2.5	A_2	5794.7035	0.0217
2	1	−1	3.5	E	1	1	−1	2.5	E	5800.5376	0.0068
2	1	1	3.5	A_2	1	1	1	2.5	A_1	5806.1112	0.0229
2	1	1	2.5	A_1	1	1	1	2.5	A_2	5841.2197	0.0083
2	1	−1	2.5	E	1	1	−1	2.5	E	5846.7933	−0.0388
2	1	1	2.5	A_2	1	1	1	2.5	A_1	5852.1586	−0.0072
2	0		1.5	E	1	0		1.5	E	5936.4921	−0.0070
2	1	1	1.5	A_1	1	1	1	2.5	A_2	6010.8764	−0.0355
2	1	−1	1.5	E	1	1	−1	2.5	E	6015.8770	−0.0277
2	1	−1	3.5	E	1	1	−1	3.5	E	6032.8583	0.0147
2	0		4.5	E	1	0		3.5	E	6131.8811	0.0432
2	0		3.5	E	1	0		2.5	E	6165.9999	0.0227
2	0		0.5	E	1	0		1.5	E	6212.8287	0.0106
2	1	1	4.5	A_1	1	1	1	3.5	A_2	6215.9020	0.0248
2	1	−1	4.5	E	1	1	−1	3.5	E	6221.8402	0.0522
2	1	1	4.5	A_2	1	1	1	3.5	A_1	6227.4138	−0.0041
2	0		2.5	E	1	0		2.5	E	6293.8284	−0.0578
2	1	1	1.5	A_1	1	1	1	1.5	A_2	6343.8867	0.0099
2	1	−1	1.5	E	1	1	−1	1.5	E	6350.1896	−0.0194
2	1	1	1.5	A_2	1	1	1	1.5	A_1	6356.2320	−0.0264
2	1	1	0.5	A_1	1	1	1	1.5	A_2	6463.1204	−0.0091
2	1	−1	0.5	E	1	1	−1	1.5	E	6468.7982	−0.0470
2	1	1	0.5	A_2	1	1	1	1.5	A_1	6474.2676	−0.0208

attempted using different values of the ν_6 fundamental frequency (see Table 4). With either choice, the authors were able to achieve very good agreement with the available data. However, the two fits yielded radically different values of the A_6 rotational constant, which is not well determined by the available microwave data. Our approach was to obtain the most physically reasonable fit model by using the results of *ab initio* force field calculations to constrain as many of the poorly determined parameters as possible.

Unfortunately, calculations performed within the Born–Oppenheimer approximation typically result in ± 10 cm^{-1} errors in vibrational frequencies so that the ν_6 frequency cannot be meaningfully constrained by the available theory. However, centrifugal distortion constants and Coriolis zeta parameters obtained from *ab initio* force fields can be quite reliable for molecules of this size. It can be more challenging to compare experimentally derived vibration-rotation constants with those obtained by applying perturbation using the cubic force field parameters,[32] particularly for higher frequency vibrations that can participate in complicated interactions with lower frequency modes. However, for the lowest-frequency vibrational states considered here, the interaction is isolated, and its analysis can be guided by *ab initio* vibration-rotation constants.

The best-fit parameters of our model are given in Table 4. Note that the reported uncertainties reflect only the statistical uncertainty in the fit and do not include systematic errors due to correlation or due to inadequacies in the model. The ground

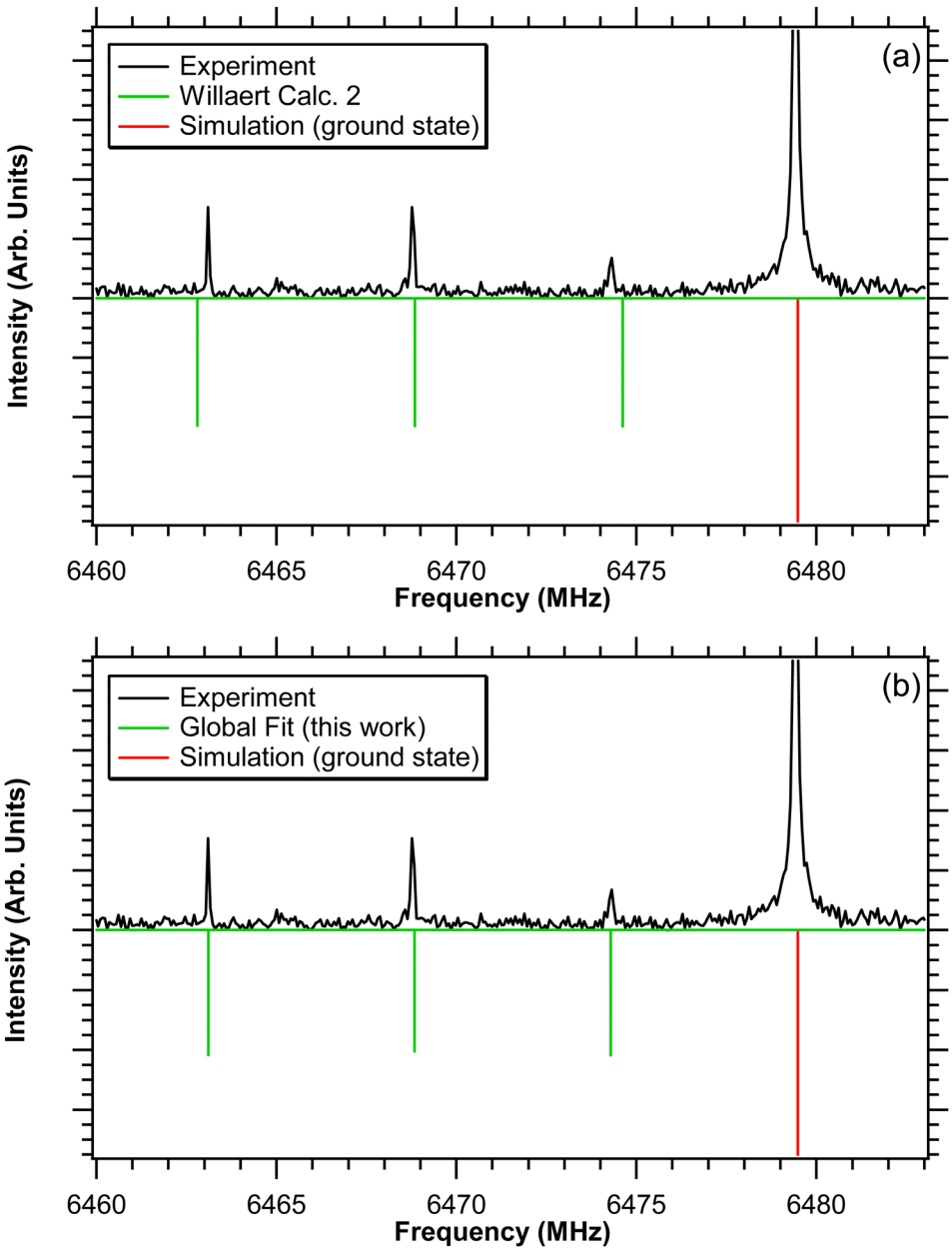

Fig. 3 The frequencies of the ν_6 vibrational satellites of the $(J,K,F) = (2,1,0.5) \leftarrow (1,1,1.5)$ transition are compared to (a) simulated line positions calculated from the fit parameters reported in Calc. 2 of Willaert *et al.*[18] and (b) simulated line positions using the parameters reported in Table 4 of this work.

state parameters were constrained to literature values obtained from microwave spectroscopy, with the exception of the D_K^0 centrifugal distortion parameter, which is not well determined by spectroscopy, but which affects the fit of the Coriolis interaction. The D_K parameter for all levels was therefore constrained to the *ab initio* value. For the ν_6 level, the A_6 rotational constant was constrained to the *ab initio* value, D_J^6 was constrained to the ground state value, and the eQq_6 nuclear quadrupole coupling constant and C_6 spin-rotation interaction constant were constrained to the literature values of ref. 15 and 17, respectively. The other parameters, including the B_6 rotational constant and the ν_6 fundamental frequency were floated. In order to fit the high-resolution *l*-type doubling transitions[17] adequately, it was necessary to include a q_J centrifugal distortion correction to the *l*-type doubling constant. The eQq_3 constant for the ν_3 level was constrained to the literature value.[15] The ν_3–ν_6 *b*-axis Coriolis matrix element was constrained using the *ab initio* $\zeta_{36}^{(b)}$ value. We attempted to include a q_K centrifugal distortion correction to the *l*-type doubling constant as well as higher order C_x^J and C_x^K centrifugal distortion corrections to the Coriolis interaction as was necessary to achieve the fits reported in ref. 18, but none of these higher order parameters improved the quality of the fit. We use the definitions of C_0 and C_6 spin-rotation parameters given in ref. 14 and 17, respectively. The $eQq\eta$ parameter is defined in the same way as the χ_6 parameter given in ref. 17. The definitions of the C_x^J and D_x^K parameters shown in Table 4 are given in ref. 18.

The fit errors are summarized in Table 5. The errors were somewhat larger than those obtained from the effective, isolated ν_6 fit (Table 3). However, the low-*J* transitions reported here, the millimeter-wave transitions of ref. 15, and the ν_3 IR data[18] are all fitted with rms errors that are smaller than or similar to the reported measurement uncertainties. The *l*-type doubling transitions reported by Gerke and Harder[17] were recorded with high frequency resolution (~1.8 kHz measurement error), but are fitted with an rms error of 7.1 kHz, indicating that the model is not capable of reproducing all observations perfectly. (The rms error for this data set obtained in the fit by Willaert *et al.*[18] was 8.4 kHz.) It was possible to achieve a better fit by floating the D_J^6 parameter, but this led to a value that was inconsistent with the force field prediction. We believe the model parameters are more physically meaningful with the constraint in place.

A list of residuals (Obs–Calc) to our new observations is printed in Table 2b. A full list of the observed transitions and their fit residuals are given in the Supplementary Information. Fig. 3b illustrates the quality of the fit to the low-*J* *l*-type doubled ν_6 vibrational sattelites reported here. The quality of the fit the ν_3 IR spectrum[18] is illustrated in Fig. 4.

Discussion

We considered the physical reasonableness of our model parameters. The D_{JK}^6, D_J^3, and D_{JK}^3 parameters were floated but differed from their ground state values by only 17 Hz, 3.6 Hz, and 9 Hz, respectively, indicating that they are not strongly perturbed by the Coriolis interaction. A comparison of other parameters to predictions of the *ab initio* force field is made in Table 6. The *ab initio* rotation-vibration constants listed in the table include the quadratic and anharmonic correction terms of ref. 32, but do not include the Coriolis correction since that interaction is treated explicitly in the model. In particular, note that our $\alpha_6^{(A)}$ parameter was constrained to match the MP2 6-311G** value, whereas the corresponding values obtained by Walters and Whiffen[15] and the two Willaert models[18] differ from the *ab initio* value by 7.7 MHz, 8.4 MHz, and −15.8 MHz, respectively. The other rotational constants were floated in our fit. The $\alpha_3^{(A)}$ and $\alpha_3^{(B)}$ vibration-rotation constants differ from the MP2 6-311G** prediction by only 24 kHz and 234 kHz, respectively. The $\alpha_3^{(B)}$ parameters in Willaert's Calc. 3[18] differs from the *ab initio* value by at least 1.5 MHz. Our $\alpha_6^{(B)}$ parameter differs from the *ab initio* value by 520 kHz, which may indicate that the B_6 rotational constant is still slightly perturbed by the interaction. In our fit, the $\zeta_{36}^{(b)}$ parameter was constrained to the MP2 value. In Willaert's Calc. 3, the discrepancy with the *ab initio* $\zeta_{36}^{(b)}$ parameter is significant, which may indicate that this model is based on unreasonable assumptions.

Our analysis of the rotational structure favors a high ν_6 value of 267.28 cm^{-1}, similar to the value reported by Walters and Whiffen[15] and the value obtained in Willaert's Calc. 2 model.[18] This value is consistent with a ν_3–ν_6 frequency difference of 19.0 cm^{-1}. This value disagrees with the value ν_6 = 261.5 ± 1.5 cm^{-1}, derived from careful consideration of the vibrational level structure.[16] In order to address this discrepancy, we performed a second fit in which ν_6 was constrained to 261.5 cm^{-1}. With this constraint, it was possible to fit the microwave (this work and ref. 17) and millimeter-wave[15] observations

Table 3 Fit parameters for ν_6 data, treating ν_6 as an isolated state. Standard errors in units of the final printed digit are given in parentheses

Parameter	This work	Ref. 15	Ref. 17
A/MHz	5760[a]	5760	
B/MHz	1520.628065(72)	1520.6281(1)	
D_J/kHz	0.16181(14)	0.16185(8)	
D_{JK}/kHz	1.1929(15)	1.1934(10)	
H_{JKK}/Hz	−0.07137(110)	−0.070(2)	
$A\zeta$/MHz	798.3(38)	787.5(39)	
η_J/kHz	−18.023(21)	−18.005(6)	
η_{JK}/Hz	−1.618(41)	−1.65(7)	
q^+/MHz	−2.93549738(37)	−2.9360(5)	2.93549750(72)
q_J/Hz	4.97256(16)	2.9(4)	−4.97260(32)
eQq/MHz	−2144.58[a]	−2144.58(12)	
$eQq\eta$/MHz	−9.0279(16)		−9.0278(32)
C_6/Hz	−81.1(16)		−84.7(31)

Dataset	Description	No. of transitions	Ave. Msmt error (kHz)	rms fit error (kHz)
Ref. 15	mm-wave, *J* = 11–46	304	240	128
Ref. 17	*l*-type doubling transitions	72	1.8	2.2
This work	*J* = 0–2	27	50	28

[a] Constrained to the value of ref. 15.

Table 4 Parameters for the global fit of the interacting ν_3–ν_6 levels

Parameters	This work	Ref. 15	Ref. 18, calc. 2	Ref. 18, calc. 3
Ground state				
A_0/MHz	5759.01[ab]	5760[a]	5759.01[a]	5759.01[a]
B_0/MHz	1523.28267[ac]	1523.28267(9)	1523.28267[a]	1523.28267[a]
D_J^0/kHz	0.16462[ac]	0.16462(2)	0.16462[a]	0.16462[a]
D_{JK}^0/kHz	0.9925[ac]	0.9925(4)	0.9925[a]	0.9925[a]
D_K^0/kHz	0.31937[ad]		0.294[a]	0.294[a]
eQq_0/MHz	−2145.207[ac]	−2145.207(3)		
C_0/kHz	6.88[ae]	4.7(6)		
ν_6 = 1				
ν_6/cm^{-1}	267.28155(33)	267.3[a]	267.65[a]	261.5[a]
A_6/MHz	5766.7266[ad]	5760[a]	5758.58175[a]	5782.4847(24)
B_6/MHz	1521.92013(21)	1522.02	1522.07788(10)	1522.5576(31)
D_J^6/kHz	0.16462[af]	0.1627	0.16462[a]	0.16462[a]
D_{JK}^6/kHz	0.9753(11)	0.9916	1.02069(330)	1.02228(150)
D_K^6/kHz	0.31937[adf]		0.294[a]	0.294[a]
$A_6\zeta_{66}^{\zeta(a)}$/MHz	793.80(50)	787.5[a]	787.5[a]	787.5[a]
η_J^6/kHz	−2.414(25)	−1.263		
q^+/MHz	−0.320319(46)	−0.1269	0	0.9597(60)
q_J/Hz	2.5523(14)		−1.295(80)	−1.232(56)
q_K/MHz			0.214(28)	
eQq_6/MHz	−2144.58[ac]	−2144.58(12)		
$eQq\eta$/MHz	−9.0212(21)			
C_6/Hz	−84.7[ag]			
ν_3 = 1				
ν_3/cm^{-1}	286.297298(32)		286.29712(3)	286.29713(5)
A_3/MHz	5758.58458(25)	5760	5758.58175(320)	5758.5799(48)
B_3/MHz	1519.70047(27)	1519.51	1519.381145(29)	1518.4218(61)
D_J^3/kHz	0.168252(20)	0.1692	0.16462[a]	0.16462[a]
D_{JK}^3/kHz	0.98347(48)	0.9915	0.94497(420)	0.94198(260)
D_K^3/kHz	0.31937[adf]		0.294[a]	0.294[a]
eQq_3/MHz	−2146.49[ac]	−2146.49(11)		
Interactions				
$\sqrt{2}B_0\Omega_{\zeta_{36}}^{\zeta(b)}$/MHz	861.4[ad]	878.6[a]	903.7567(340)	1201.113(940)
C_x^J/kHz			−0.79255(410)	−1.55868(720)
C_x^K/kHz			−4.767(350)	−5.831(180)

[a] Constrained values. [b] Ref. 25. [c] Ref. 15. [d] MP2 6-311G**. [e] Ref. 14. [f] Ground state value. [g] Ref. 17.

Table 5 Summary of errors in the global fit shown in Table 4

Dataset	Description	No. of transitions	Ave. Msmt error	rms fit error
Ref. 18	IR data, ν_3 fundamental	3053	5.48×10^{-4} cm^{-1}	3.03×10^{-4} cm^{-1}
Ref. 15	mm-wave, J = 11–46	441	259 kHz	273 kHz
Ref. 17	l-type doubling transitions	72	1.8 kHz	7.1 kHz
This work	J = 0–2	27	50 kHz	28 kHz

with rms errors of 22 kHz and 350 kHz, respectively, and the high-resolution ν_3 IR data[18] with an rms error of 2.8×10^{-4} cm^{-1}. This fit required the use of high-order C_x^J and C_x^K corrections to the Coriolis interaction matrix elements, similar to the ones obtained in the Calc. 3 model of Willaert *et al.*[18] Similar to the Calc. 3 model, the fit leads to a high value of A_6 = 5785.58 cm^{-1}, and it leads to a $\zeta_{36}^{(b)}$ value of 0.5570, which is 40% higher than the value obtained from the harmonic force field. For these reasons, the perturbed rotational structure appears to be more naturally consistent with the high ν_6 value. However, the fact that a good fit can be achieved with both ν_6 values clearly demonstrates correlation among the model parameters. Indirect determination of the ν_6 frequency by our fitting model is inconclusive, and we cannot rule out the lower value that is favored by analysis of the vibrational level structure.

Conclusion

We have evaluated the performance of a newly constructed CP-FTMW spectrometer, demonstrating that we can readily

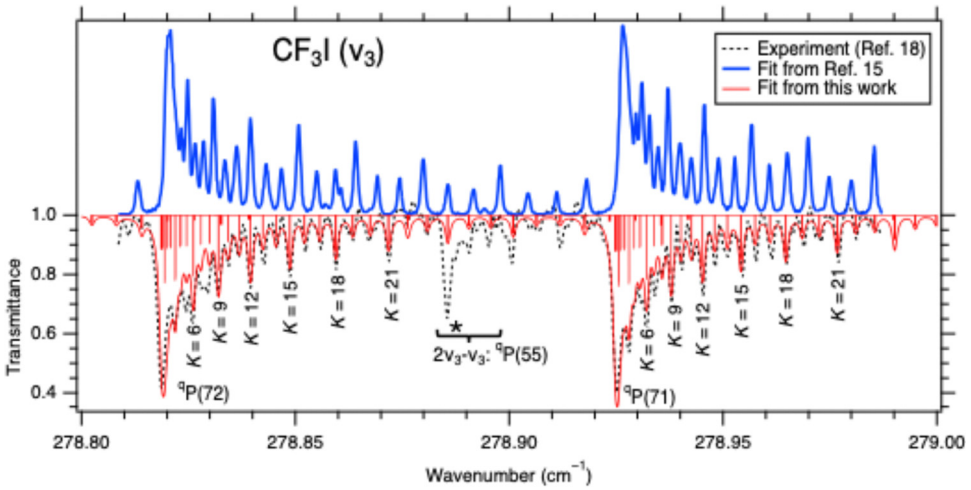

Fig. 4 The recorded spectrum of the $^{q}P(71)$ and $^{q}P(72)$ branches of the ν_3 fundamental transition[18] (dotted line) is compared with the simulated spectra predicted by our fit (thin red line, downward directed peaks) and with the simulated spectrum predicted by the parameters of Walters and Whiffen[15] (thick blue line, upward directed peaks). The Walters and Whiffen prediction exhibits disagreement with the IR measurements at high J and high K because it is based on data that only extended to J = 41. Note that the feature at ~278.886 cm^{-1} (maked with an asterisk) is due to the $2\nu_3-\nu_3$ hot band which is omitted from the fit model.

Table 6 Comparison of parameters derived from the fit (Table 4) with *ab initio* values obtained from the force field calculation

Parameters	This work	Ref. 15	Ref. 18, calc. 2	Ref. 18, calc. 3	MP2 6-311G**	CCSD 6-311G**	CCSD(T) 6-311G**
D_J^0/kHz	0.16462[a]	0.16462(2)	0.16462[a]	0.16462[a]	0.1588	0.1580	0.1641
D_{JK}^0/kHz	0.9925[a]	0.9925(4)	0.9925[a]	0.9925[a]	0.8552	0.8611	0.8703
D_K^0/kHz	0.31937[a]		0.294[a]	0.294[a]	0.31937	0.3097	0.3100
$\alpha_6^{(A)}$/MHz	−7.7166[a]	0[a]	0.42825[a]	−23.4747(24)	−7.7166	−7.864	
$\alpha_6^{(B)}$/MHz	1.36254(21)	1.26	1.2048(1)	0.7251(31)	0.8424	0.8529	
$\zeta_{66}^{(a)}$	0.13765(9)	0.1367	0.1368[a]	0.1362[a]	0.1319	0.1319	0.1341
$\alpha_3^{(A)}$/MHz	0.4254(3)	0[a]	0.4283(32)	0.4301(48)	0.4017	0.3747	
$\alpha_3^{(B)}$/MHz	3.5822(3)	3.77	3.90153(3)	4.8609(61)	3.3487	3.2977	
$\zeta_{36}^{(b)}$	0.3996[a]	0.4076[a]	0.41928(2)	0.5570(4)	0.3996	0.3945	0.3963

[a] Constrained value.

observe vibrational satellites and ^{13}C peaks in natural abundance. We have re-evaluated the spectroscopic constants for the interacting ν_3 and ν_6 vibrational levels of CF_3I, and we have obtained an updated fit to the complete set of frequencies reported here and in the literature. Although our analysis favors a high ν_6 value of 267.28 cm^{-1}, the evidence is insufficient to rule out the lower value of ν_6 = 261.5 cm^{-1}, obtained from evaluation of the vibrational level structure.

Data availability

The data supporting this article have been included as part of the ESI.†

Conflicts of interest

There are no conflicts to declare.

Acknowledgements

This material is based upon work supported by the National Science Foundation under Grant No. 2340303. G. B. P. is grateful to Bob Field for generously donating some of the equipment used to build the preliminary Chirped Pulse spectrometer described in this work. The authors thank Agnès Perrin and Laurent Manceron for graciously providing us with a list of their observed frequencies for the ν_3 fundamental transition. Open Access funding provided by the Max Planck Society.

References

1 J. Zhang, D. J. Wuebbles, D. E. Kinnison and A. Saiz-Lopez, Revising the Ozone Depletion Potentials Metric for Short-Lived Chemicals Such as CF_3I and CH_3I, *J. Geophys. Res.: Atmos.*, 2020, **125**, e2020JD032414, DOI: 10.1029/2020JD032414.

2 Y. Kobayashi and I. Kumadaki, Trifluoromethylation of aromatic compounds, *Tetrahedron Lett.*, 1969, **10**, 4095–4096, DOI: 10.1016/S0040-4039(01)88624-X.
3 Y. He, J. Pochert, M. Quack, R. Ranz and G. Seyfang, Dynamics of unimolecular reactions induced by monochromatic IR radiation: experiment and theory for $C_nF_mH_kI \rightarrow C_nF_mH_k + I$ probed with hyperfine-, Doppler- and uncertainty-limited time resolution of iodine-atom IR absorption, *Faraday Discuss.*, 1995, **102**, 275–300, DOI: 10.1039/FD9950200275.
4 W. F. Edgell and C. E. May, Raman and Infrared Spectra of CF_3Br and CF_3I, *J. Chem. Phys.*, 1954, **22**, 1808–1813, DOI: 10.1063/1.1739925.
5 R. J. H. Clark and O. H. Ellestad, The vapour phase Raman spectra, Raman band contour analyses, Coriolis coupling constants, and *e*-species force constants for the molecules HCF_3, $ClCF_3$, $BrCF_3$, and ICF_3, *Mol. Phys.*, 1975, **30**, 1899–1911, DOI: 10.1080/00268977500103371.
6 W. B. Person, S. K. Rudys and J. H. Newton, Absolute integrated infrared absorption intensities of trichlorofluoromethane and trifluoroiodomethane fundamentals in the gas phase. Intensity sum rule, *J. Phys. Chem.*, 1975, **79**, 2525–2531, DOI: 10.1021/j100590a016.
7 W. Fuss, Fundamental and overtone infrared spectra of CF_3I, *Spectrochim. Acta, Part A*, 1982, **38**, 829–840, DOI: 10.1016/0584-8539(82)80102-5.
8 F. Kohler, H. Jones and H. D. Rudolph, Laser-microwave double-resonance spectroscopy in CF_3I with four CO_2-laser lines, *J. Mol. Spectrosc.*, 1980, **80**, 56–70, DOI: 10.1016/0022-2852(80)90270-2.
9 J. G. McLaughlin, M. Poliakoff, J. G. Smith and S. Walters, Direct observation of the ν_6 band in the IR spectrum of CF_3I dissolved in liquid xenon, *J. Mol. Struct.*, 1983, **102**, 289–293, DOI: 10.1016/0022-2860(83)85066-2.
10 J. Sheridan and W. Gordy, The Microwave Spectra and Molecular Structures of Trifluoromethyl Bromide, Iodide, and Cyanide, *J. Chem. Phys.*, 1952, **20**, 591–595, DOI: 10.1063/1.1700499.
11 F. Sterzer, $J = 0 \rightarrow 1$ Rotational Transition of Trifluoroiodomethane, *J. Chem. Phys.*, 1954, **22**, 2094, DOI: 10.1063/1.1740013.
12 H. Jones and F. Kohler, Infrared-microwave double resonance in CF_3I; Microwave spectroscopy in emission and absorption, *J. Mol. Spectrosc.*, 1975, **58**, 125–141, DOI: 10.1016/0022-2852(75)90161-7.
13 A. P. Cox, G. Duxbury, J. A. Hardy and Y. Kawashima, Microwave spectra of CF_3Br and CF_3I. Structures and dipole moments, *J. Chem. Soc., Faraday Trans. 2*, 1980, **76**, 339–350, DOI: 10.1039/F29807600339.
14 S. L. Stephens and N. R. Walker, Determination of nuclear spin–rotation coupling constants in CF_3I by chirped-pulse Fourier-transform microwave spectroscopy, *J. Mol. Spectrosc.*, 2010, **263**, 27–33, DOI: 10.1016/j.jms.2010.06.007.
15 S. W. Walters and D. H. Whiffen, Rotational spectrum of trifluoroidomethane, *J. Chem. Soc., Faraday Trans. 2*, 1983, **79**, 941–949, DOI: 10.1039/F29837900941.
16 H. Bürger, K. Burczyk, H. Hollenstein and M. Quack, High resolution FTIR spectra of $^{12}CF_3I$, $^{13}CF_3I$ and $^{12}CF_3{}^{79}Br$ near 1050 cm^{-1} and 550 cm^{-1}, *Mol. Phys.*, 1985, **55**, 255–275, DOI: 10.1080/00268978500101311.
17 C. Gerke and H. Harder, Direct *l*-type doubling transitions in the $\nu_6 = 1$ vibrational state of CF_3Br and CF_3I: *l*-type resonance effects on the spin-rotation coupling, *Chem. Phys. Lett.*, 1996, **255**, 287–294, DOI: 10.1016/0009-2614(96)00399-5.
18 F. Willaert, P. Roy, L. Manceron, A. Perrin, F. Kwabia-Tchana, D. Appadoo, D. McNaughton, C. Medcraft and J. Demaison, High resolution investigation of the ν_3 band of trifluoromethyliodide (CF_3I), *J. Mol. Spectrosc.*, 2015, **315**, 16–23, DOI: 10.1016/j.jms.2014.12.021.
19 G. G. Brown, B. C. Dian, K. O. Douglass, S. M. Geyer, S. T. Shipman and B. H. Pate, A broadband Fourier transform microwave spectrometer based on chirped pulse excitation, *Rev. Sci. Instrum.*, 2008, **79**, 053103, DOI: 10.1063/1.2919120.
20 G. B. Park and R. W. Field, Perspective: The first ten years of broadband chirped pulse Fourier transform microwave spectroscopy, *J. Chem. Phys.*, 2016, **144**, 200901, DOI: 10.1063/1.4952762.
21 J. L. Neill, S. T. Shipman, L. Alvarez-Valtierra, A. Lesarri, Z. Kisiel and B. H. Pate, Rotational spectroscopy of iodobenzene and iodobenzene–neon with a direct digital 2–8 GHz chirped-pulse Fourier transform microwave spectrometer, *J. Mol. Spectrosc.*, 2011, **269**, 21–29, DOI: 10.1016/j.jms.2011.04.016.
22 D. Schmitz, V. Alvin Shubert, T. Betz and M. Schnell, Multi-resonance effects within a single chirp in broadband rotational spectroscopy: The rapid adiabatic passage regime for benzonitrile, *J. Mol. Spectrosc.*, 2012, **280**, 77–84, DOI: 10.1016/j.jms.2012.08.001.
23 CFOUR, a quantum chemical program package written by J. F. Stanton, J. Gauss, L. Cheng, M. E. Harding, D. A. Matthews, P. G. Szalay with contributions from A. Asthana, A. A. Auer, R. J. Bartlett, U. Benedikt, C. Berger, D. E. Bernholdt, S. Blaschke, Y. J. Bomble, S. Burger, O. Christiansen, D. Datta, F. Engel, R. Faber, J. Greiner, M. Heckert, O. Heun, M. Hilgenberg, C. Huber, T.-C. Jagau, D. Jonsson, J. Jusélius, T. Kirsch, M.-P. Kitsaras, K. Klein, G. M. Kopper, W. J. Lauderdale, F. Lipparini, J. Liu, T. Metzroth, L. A. Mück, T. Nottoli, D. P. O'Neill, J. Oswald, D. R. Price, E. Prochnow, C. Puzzarini, K. Ruud, F. Schiffmann, W. Schwalbach, C. Simmons, S. Stopkowicz, A. Tajti, T. Uhlířová, J. Vázquez, F. Wang, J. D. Watts, P. Yergün, C. Zhang, X. Zheng and the integral packages MOLECULE (J. Almlöf and P. R. Taylor), PROPS (P. R. Taylor), ABACUS (T. Helgaker, H. J. Aa. Jensen, P. Jørgensen, and J. Olsen), and ECP routines by A. V. Mitin and C. van Wüllen. For the current version, see https://www.cfour.de.
24 R. Krishnan, J. S. Binkley, R. Seeger and J. A. Pople, Self-consistent molecular orbital methods. XX. A basis set for correlated wave functions, *J. Chem. Phys.*, 1980, **72**, 650–654, DOI: 10.1063/1.438955.

25 V. Typke, M. Dakkouri and H. Onerhammer, On the molecular structure of X-CF_3 molecules (X = Cl, Br, I), *J. Mol. Struct.*, 1978, **44**, 85–96, DOI: 10.1016/0022-2860(78)85008-X.
26 Y. He, H. Hollenstein, M. Quack, E. Richard, M. Snels and H. Bürger, High resolution analysis of the complex symmetric CF_3 stretching chromophore absorption in CF_3I, *J. Chem. Phys.*, 2002, **116**, 974–983, DOI: 10.1063/1.1370948.
27 Y. Matsumoto, M. Takami and P. A. Hackett, High-resolution infrared absorption spectroscopy of the CF_3I ν_2 band, *J. Mol. Spectrosc.*, 1986, **118**, 310–312, DOI: 10.1016/0022-2852(86)90244-4.
28 P. B. Davies, N. A. Martin and M. D. Nunes, Diode laser spectroscopy of the 4^1_0 band of $^{12}CF_3I$ and $^{13}CF_3I$ in a supersonic jet, *Spectrochim. Acta, Part A*, 1989, **45**, 293–298, DOI: 10.1016/0584-8539(89)80136-9.
29 H. M. Pickett, The fitting and prediction of vibration-rotation spectra with spin interactions, *J. Mol. Spectrosc.*, 1991, **148**, 371–377, DOI: 10.1016/0022-2852(91)90393-O.
30 S. W. Walters and D. H. Whiffen, Supplementary Publication No. SUP 23561, The British Library, 1983.
31 G. Tarrago and S. Maes, Influence de la vibration sur la structure hyperfine des niveaux de rotation des molécules à symétrie ternaire, *C. R. Seances Acad. Sci., Ser. 2*, 1968, **266**, 699.
32 I. M. Mills, in *Molecular Spectroscopy: Modern Research*, ed. K. N. Rao and C. W. Mathews, Academic Press, New York, 1972, p. 115.